PROCEEDINGS OF SCIENCE

# Performance and Operation of the ATLAS Resistive Plate Chambers Detector in 2011

**Alessandro Polini***
*INFN Bologna*
*E-mail:* alessandro.polini@bo.infn.it

**on behalf of the ATLAS Collaboration**

Resistive Plate Chambers provide the barrel region of the ATLAS detector with an independent muon trigger and a two-coordinate measurement. The chambers, arranged in three concentric double layers are operated in a strong magnetic toroidal field and cover a surface area of about $4000\,m^2$. During 2011 the LHC has provided proton-proton collisions at 7 TeV in the center-of-mass frame with a steady increase in instantaneous luminosity over several orders of magnitude, summing up to about 5 $fb^{-1}$. The operational experience for this running period is presented along with studies of the detector performance as a function of luminosity, environmental conditions and working point settings. The measurements presented allow the planning of a strategy for the data taking in the next years and make some predictions about the performance with higher luminosities.

*XI workshop on Resistive Plate Chambers and Related Detectors - RCP2012,*
*February 5-10, 2012*
*INFN Laboratori Nazionali di Frascati Italy*

*Speaker.

 

PoS(RPC2012)006

## 1. Introduction

In 2011 the bulk of the LHC program has provided proton-proton collisions at a centre of mass energy of 7 TeV with instantaneous luminosities up to $3.65 \times 10^{33}\, cm^{-2}s^{-1}$, totaling an integrated luminosity of $5.6\, fb^{-1}$. In addition the last month of the 2011 running also provided $166\, \mu b^{-1}$ of lead-lead nuclei collisions. This document presents the performance and operational experience of the detector in this period. The document is organized as follows. After a brief description of the ATLAS Resistive Plate Chambers (RPCs), the detector status along with results from coverage and trigger performance are presented. Details of operational experience along with studies of the detector performance as a function of luminosity, environmental conditions and working point settings are shown in Section 4. Improvements and upgrade activities are described in Section 5. Finally some concluding remarks and outlook are given in Section 6.

## 2. The ATLAS Resistive Plate Chambers

RPCs[1] provide the barrel region of the ATLAS detector [2] with an independent muon trigger and a two-coordinate measurement. The chambers are arranged in three concentric double layers (middle confirm, pivot, outer confirm) and are operated in a strong magnetic toroidal field and cover a surface area of about 4000 $m^2$. A low $p_T$ ($< 10$ GeV) trigger requires a projective coincidence between hits in the pivot and the middle confirm layer while high $p_T$ triggers require hits also in the outer confirm layer.

An ATLAS RPC is made of 2 layers, each with two 2 mm thick bakelite laminate plates and providing 2 $\eta$ and 2 $\phi$ strip planes. Made of phenolic and melaminic resins, the plates are kept apart at 2 mm by insulating spacers, enclosing a gas volume filled with a mixture of $C_2H_2F_4$(94.7%) - $C_4H_{10}$ (5%) - $SF_6$ (0.3%). The external surface of the plates is coated with a thin layer of graphite paint to allow a uniform distribution of the high voltage along the plates. The smoothness of the inner surfaces is enhanced by means of a thin layer of linseed oil. The high voltage (HV) working point is chosen to be at 9.6 kV at a temperature of $24°C$ and a pressure of 970 mbar. In these conditions the RPCs work in saturated avalanche mode inducing, for a minimum ionizing particle, a prompt charge of about 1 pC on the pick-up strips and delivering in the gas an average total charge of 30 pC. The discharge electrons drift in the gas and the signal, induced on pick-up copper strips, is read out via capacitive coupling, and detected by the front-end electronics. Read-out strips have a typical width of $\sim 30$ mm and are grouped in two ($\eta$ and $\phi$) read-out panels with strips orthogonal to each other. Custom front-end electronics amplifies, discriminates and converts the detector signals to ECL standard. These signals are passed to the on-detector trigger electronics[3] which, by requiring appropriate coincidences in the $\eta$ and $\phi$ detector layers, provide ATLAS with a Level 1 trigger decision along with the detector data for accepted events.

## 3. Detector Status and Performance

The 2011 data taking has been very successful for the RPC system which has been running with a fraction of active readout channels of 97% (out of a total of 370 k) and an average active trigger area of $99 \sim 99.5$%. The number of gas volumes either disconnected or operated not at

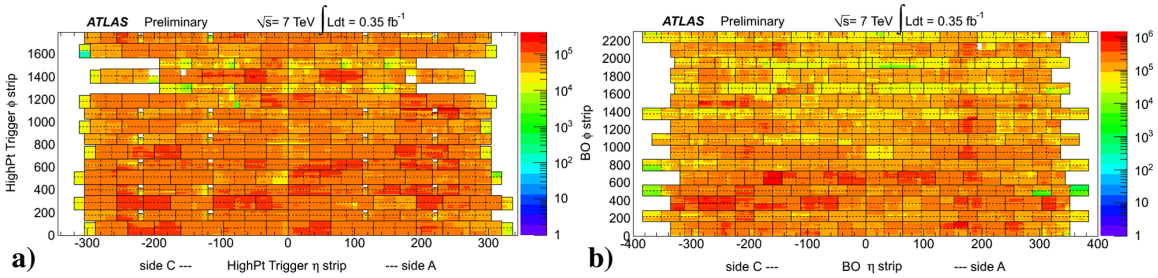


**Figure 1: a)** The spatial coincidence between $\eta$ and $\phi$ RPC pivot strips generating a High $p_T$ trigger threshold in terms of pseudo-rapidity and azimuthal angle coordinates, respectively. **b)** The spatial coincidence between $\eta$ and $\phi$ strips of the outer double layer (RPC BO). Shown are data from the Muon_Physics stream taken between March and May 2011 when detector and beam flags were green.

nominal conditions has been below 2% with 47 (out of 3592) being off due to broken gas inlets and 23 being kept at lower voltage for recovery due to bad gas supply or too high currents. The physics data taking has been stable with around 99% of the collected data flagged as good for physics analyses. Fig. 1 shows the detector coverage in strip units for the whole 2011 proton run. The plots reflect the detector chamber structure and coverage. The plots show a uniform coverage both for the trigger and the detector hits. The empty regions around $\phi$ strip 1400 and the 2 surrounding sectors come from the different design of the ATLAS detector in the lower sectors where the infrastructure to sustain the whole detector and the access paths for maintenance are located. Fig. 2a presents the efficiency per gas volume and compares the performance of 2011 with the one in 2010. As can be seen an important improvement was achieved in 2011 coming mainly from:

- the dynamic adjustment of the high voltage working point as a function of the local environmental conditions (temperature and atmospheric pressure).
- a general detector consolidation
- precise timing calibration

On the working point adjustment more details are given in section 4. The plot in Fig. 2b shows the RPC timing performance. The profile is sharp and centered in the middle of the readout window indicating that the RPCs can be used as a precise timing system[4].

Fig. 3a shows the trigger efficiency as a function of the muon transverse momentum $p_T$. Six different trigger slots with increasing momentum threshold as they are provided online by the RPC trigger system are displayed. The plateau efficiency is around 80% for low-$p_T$ triggers (4, 6, 10 GeV) as expected as it includes also the detector geometric acceptance. For the high-$p_T$ triggers (11, 15, 20 GeV) the efficiency plateau is around 70% as the trigger requires a coincidence also in the outer plane further reducing the geometric acceptance. The effect of the detector acceptance is clearly seen when plotting the efficiency as a function of $\phi$ as seen in Fig.3b. The region with 2 dips corresponds to the lower ATLAS sectors where the support of the whole detector is located and where some chambers are missing to allow access inside the detector. In addition to this, the structure with small even and large odd sectors following the 8 large toroidal coils over $\phi$ can be also seen.

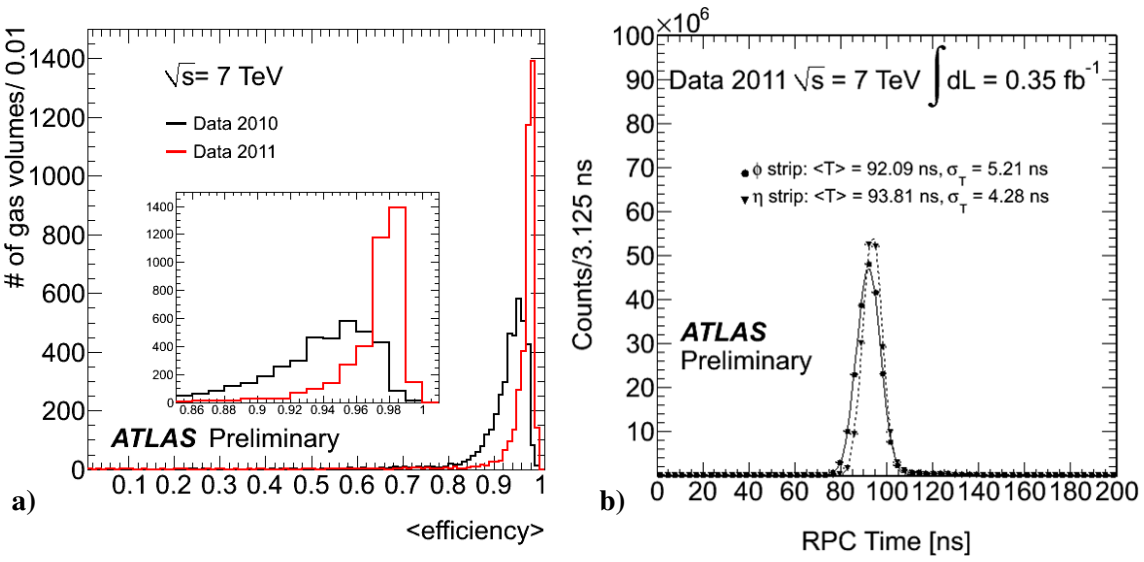


**Figure 2: a)** The distribution of the measured 2010 and 2011 RPC gas volume efficiencies defined by the positive response of at least one of the two views. The data correspond to all Muon Physics stream data for both years when detector and beam flags were green. **b)** The distribution of 2011 RPC time in readout hits for both views. No off-line time correction is applied and the time spread is dominated by the spread of signal propagation along the strip which can be corrected off-line. The data correspond to all Muon Physics stream data for both years when detector and beam flags were green

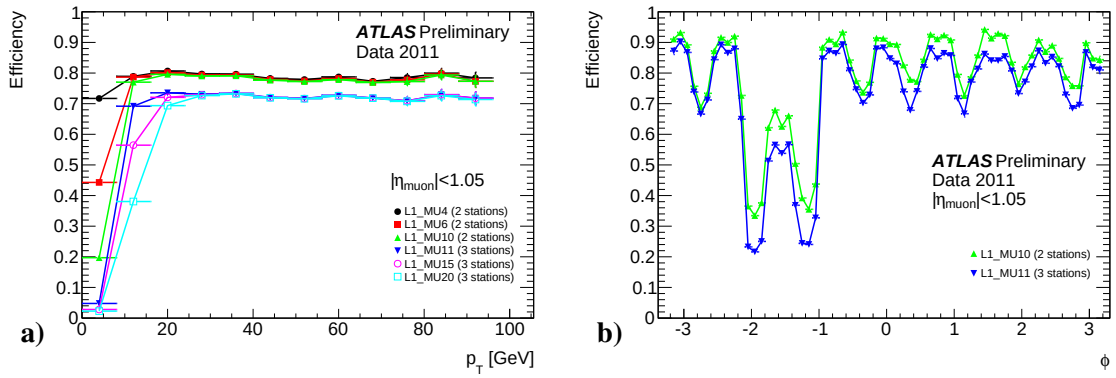


**Figure 3: a)** L1 Barrel Trigger Efficiency with respect to combined muon reconstruction (as a function of $p_T$) L1 muon barrel trigger efficiency, for the six nominal thresholds, with respect to offline reconstructed muon as a function of the muon $p_T$. The different acceptance between the 2-station coincidence low-$p_T$ thresholds (MU4, MU6, MU10) and the 3-station coincidence high-$p_T$ thresholds (MU11, MU15, MU20) is caused by the smaller coverage for the additional coincidence. **b)** The L1 muon barrel trigger efficiency, for the 2-station threshold MU10 and the 3-station threshold MU11, with respect to offline reconstructed combined muon, selected with $p_T > 15$ GeV and as a function of $\phi$. The efficiency has been determined with a tag and probe method using di-muon events. The data used correspond to total integrated luminosity of 380 $pb^{-1}$.

During 2011 the bulk of the proton collisions have been taken with 50 ns bunch spacing following the fact that the LHC was able to achieve higher luminosity and beam stability with respect to the running with 25 ns bunch spacing. Running with higher bunch spacing means that concurrently at equal luminosity the pileup ($\mu$) increases and effects on detector efficiency, or linearity and saturation effects might come into the game.

Fig.4 shows the RPC trigger performance as a function of the pileup $\mu$. Data corresponds to the period of highest luminosity with an average pileup $< \mu >$ of 15. No significant dependence on the RPC trigger efficiency is observed.

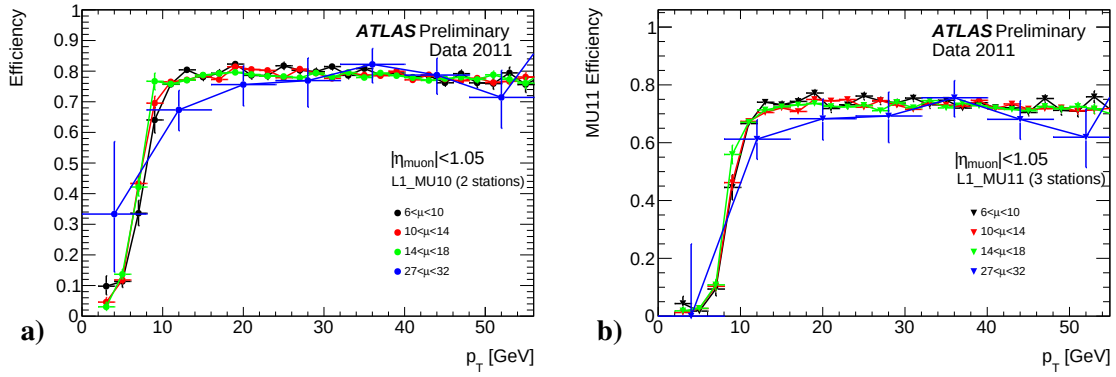


**Figure 4:** The L1 muon barrel trigger efficiency, for the 2-station threshold MU10 **(a)** and for the 3-station threshold MU11 **(b)**, with respect to offline reconstructed combined muon as a function of the muon $p_T$. The efficiency curves are shown for different ranges of the average number of interactions per bunch crossing, $\mu$. The efficiency has been determined with a tag and probe method using di-muon events. The data used correspond to total integrated luminosity of 380 $pb^{-1}$.

## 4. Detector Operation and Running Peculiarities

The year 2011 coincided with the introduction of several automatic monitoring and control tools to simplify the detector operation and optimize the data taking conditions. The number of shifters was reduced to a single person taking care of the whole ATLAS muon system which includes also trigger chambers in the endcap region and precision chambers[2].

One further improvement was to add to the RPC Detector Control System the full automatic control of the HV settings. These are automatically adjusted

- to follow the different LHC beam phases from injection, stable beams, to the final dump
- to compensate for the local changes of the environmental conditions (mainly local temperature and atmospheric pressure)
- to automatically check the individual gas-gaps currents, recalibrate at each end of fill the pedestals
- provide an online measurement of the cavern background rates and an instantaneous luminosity

The DCS is in charge of safely operating and monitoring the detector power system including the detector HV and LV supply. In the RPC DCS[5], a large number of settings (DAC $\sim$ 4000) and monitoring (ADC $\sim$ 6500) channels has been integrated into the system to optimize the detector performance and allow a fine monitoring at the level of the single individual RPC gas gap ($\sim$ 3600). The remaining ADC channels are used to monitor with high granularity the current draw of the front end electronics and RPC gas and environmental sensors (temperature, atmospheric pressure, relative humidity and gas flow). The ability to control by tuning thresholds, and monitoring the current of each RPC gap has shown to be very powerful for the detector operation both for tracing problems and fine tune the detector. This is particularly important as the RPC performance and aging is strongly related to the environmental parameters, namely the temperature ($T$), the atmospheric pressure ($P$), and the relative humidity. The gas gain, the noise rate and the dark current of the chamber depend on these parameters following the formula: $V_{\rm appl} = V_{\rm eff} \cdot (T_0/T) \cdot (P/P_0)$ where $V_{\rm appl}$ is the applied voltage, $T$, $P$ are the environment measurements and $T_0$, $P_0$, $V_{\rm eff}$ are the reference environmental values and HV settings. An example of the HV working point correction as a function of time is shown in Fig.5. From the beginning of 2011, the environmental information available within the DCS has been stably used allowing a general improvement in the detector performance and efficiency.

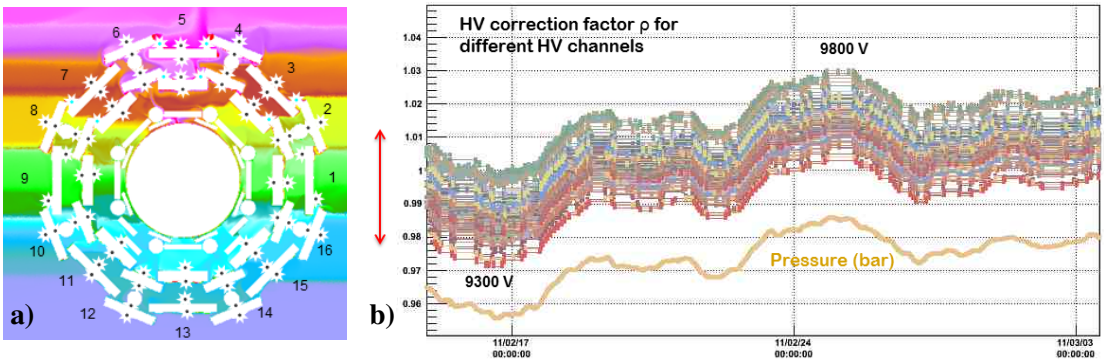


**Figure 5:** An example of the environmental correction to the RPC HV working point. The voltage of a bunch of HV channels is shown as a function of time. Chambers belonging to different detector areas being at different temperatures show a spread in the applied voltage of up to $\pm 150V$. In normal operation the temperature differences remain constant while continuous adjustment follows the trend of atmospheric pressure moving the operating voltage by up to the 3% of the nominal voltage.

The size and high granularity of the information read out and archived by the DCS is a valuable source of data for detector physics. The currents in the gas-gaps of the RPCs, measured by the DCS with a sensitivity of 2nA, allow for a precise estimation of background and beam effects. The monitored currents, environmental variables corrected and pedestals subtracted are used to estimate average currents per surface unit to study beam background and activation effects. Fig.6a shows the distributions over the longitudinal coordinate $z$ of the currents as measured and normalized by the detector surface for the 3 double layers of RPC chambers. Higher currents are observed at larger $\pm z$, as expected due to the cracks between the barrel and endcap calorimeters. The obtained distributions are in agreement with Monte Carlo simulations (not shown) and provide a good means to estimate background and detector occupancies when running at nominal LHC or upgrade

luminosities. A good correlation of the total instantaneous RPC gap currents versus the luminosity is observed allowing the RPCs to provide an independent luminosity measurement along with expectation of detector performance in the years to come. Further results and detector studies on luminosity and background measurements using the ATLAS RPC can be found in references[6, 7].

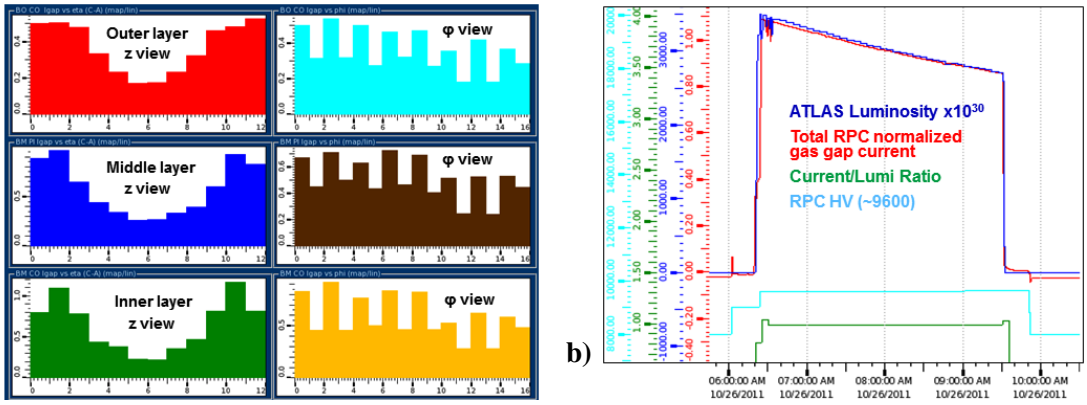


**Figure 6:** **a**) DCS online plots displaying the pedestal subtracted gas-gap currents (per unit area) for the 3 layers of RPC chambers. The views in $z$ and $\phi$ are shown. **b)** The weighted sum over the whole detector is shown together with the ATLAS instantaneous luminosity. The ratio between the two quantities is remarkably constant allowing, once calibrated, for an independent online luminosity measurement and studies on cavern activation background at beam dump.

## 5. Shutdown Activities

Those subsystems which did show some weaknesses during the running period have undergone a general overhaul during the following shutdown. Here the main activities are listed.

- Main Power Distribution:
  During the 2011 operation four occasions of partially melted Anderson-Power connectors on the 48 V power or service lines were found. After the first failures which occurred after a maintenance period, an improved monitoring of the current draw via DCS helped to avoid luminosity loss and plan controlled interventions before connector breakdown. During the shutdown a new power distribution scheme was implemented: the power connections of all systems with high draw were doubled and a daisy chain distribution scheme was abandoned in favour of a star connection.

- High Voltage Connectors:
  During the second half of the running period a few HV connectors started failing. The connectors, all located on rack side were replaced quickly in shadow accesses usually causing no direct dead area thanks to the detector double layer redundancy. Studies of the failed connectors and on unused spares from the same batch indicated a problem in the temperature cycle during the production of the insulator. The full refurbishment of the connectors on the rack side was commissioned during present shutdown.

- Gas System Consolidation:
  Some effort was put in the repair of some of the gas volumes with problematic flow. For

some chambers where leaks due to broken inlets could not be fixed a reversal of the gas flow was performed. In addition a new scheme with individually tuned impedances as function of the chamber volume and the expected integrated radiation was installed across the whole detector[8].

## 6. Conclusions

The ATLAS RPC have worked very well in 2011 delivering good trigger and data for physics. The detector redundancies along with the extensive large monitoring capabilities allowed to promptly overcome a few weak points in the infrastructure and provide valuable data for the running at higher luminosities. The consolidation activities performed during the shutdown shall further improve the stability and the detector performance for the running in 2012 and beyond.

## References

[1] R. Santonico R. Cardarelli: "Development of resistive plate counters", NIM A, 187 (1981) 377.

[2] ATLAS Muon Collaboration, "ATLAS Muon Spectrometer Technical Design Report", CERN/LHCC/97-22, (1997)

[3] F. Anulli *et al.*, "The Level-1 Trigger Muon Barrel System of the ATLAS experiment at CERN", 2009 JINST 4 P04010

[4] G. Chiodini, "The ATLAS RPC time-of-flight performance", RPC 2012, Frascati 2012, these proceedings

[5] A. Polini, "Design and Performance of the Detector Control System of the ATLAS Resistive-Plate-Chamber Muon Spectrometer", doi:10.1016/j.nima.2010.08.006

[6] M. Bindi, "ATLAS RPC detector as Luminosity monitor", RPC 2012, Frascati 2012, these proceedings

[7] G. Aielli, "Cavern background measurement with the ATLAS RPC system", RPC 2012, Frascati 2012, these proceedings

[8] E. Pastori, "The ATLAS RPC Gas Distribution", RPC 2012, Frascati 2012, these proceedings